

Keywords: rail vehicle, differential gear, running gear, dynamics, wear, simulation

Rafał MELNIK*, **Bogdan SOWIŃSKI**
Warsaw University of Technology, Faculty of Transport
Koszykowa 75, 00-662 Warsaw, Poland
*Corresponding author. E-mail: rme@wt.pw.edu.pl

ANALYSIS OF DYNAMICS OF A METRO VEHICLE MODEL WITH DIFFERENTIAL WHEELSETS

Summary. The operating conditions of light rail vehicles (trams, metro vehicles) are predominantly different compared with those of passenger or freight trains. The increased number of low-radius curves has a negative effect on wheel–rail interaction. The general design of light rail vehicle running gear is inherited from passenger trains and adapted to different loads. However, conventional solutions of a running gear may not provide smooth low-radius curve negotiation in all circumstances. In addition, a two-point contact is likely to occur, which, in turn, leads to accelerated wear of not only the wheels' tread but also their flanges. One of the proposals to deal with problems associated with the wheel–rail interaction in tight curves is implementing an automotive solution: a differential gear. The aim of the study is to investigate the dynamic behavior of a metro vehicle model equipped with differentials at each wheelset. The differentials were tested in two main variants: open and with internal friction torque. Internal friction torque value was set, consecutively, up to 2000 Nm. The results have shown that on tight curves a differential may improve rail vehicle wheel–rail interaction.

1. INTRODUCTION

In the recent years a rapid development of light railways such as trams and the metro has been observed. Many cities are building new lines or restoring defunct ones (e.g. in Europe and USA) to cope with the increasing number of citizens and commuters. These actions comply with global tendencies to limit road space for cars in favour of mass and bicycle transport. However, the new and existing lines are often routed in order to fit a dense urbanistic plan, both overground and underground. Tight buildings, especially in Europe, impose designing lines with numerous low-radius curves. From the point of view of rail vehicle operation, providing a proper interaction between a rail wheel and a track is a great challenge. The classic running gears of light rail vehicles, consisting of pivoting or non-pivoting bogies with two wheelsets, may not provide smooth tight-curve negotiating. In the case of an unconstrained wheelset (not mounted to a vehicle) curve negotiation is possible because of lateral displacement of the wheelset and conicity of the wheel tread. When passing a curve, the wheelset is shifted laterally to the outside of the curve and the rolling radii of left and right wheel change by the same value. The theoretical analysis of wheelset curving was presented by Redtenbacher in 1855 [1]. However, to achieve pure rolling of the wheelset at least one of two conditions should be met: the radius of curvature or the flangeway clearance is sufficiently large [2]. If none of the conditions is met, the wheel flange climbs the rail head and a so-called two-point or even multi-point contact occurs [3].

The design and layout of light rail vehicles is inherited from conventional rail vehicles that usually operate at higher speeds and on lines with curves of greater radii. One way to improve wheel–rail interaction on a tight curve is reducing the wheel diameter. In this solution the required difference in

rolling radii Δr is lower than that in case of large-diameter wheels. At the same time, a lower floor level is achieved, which, in turn, plays a major role in case of trams and, thus, in passenger convenience. The other actions undertaken to improve wheelset negotiation are, for example, as follows:

- track gauge widening,
- track cant,
- rail or wheel flange lubrication,
- radial wheelset steering.

However, track gauge widening and track cant may not be sufficient to reduce adverse interaction between the wheel and rail. Inadequate track widening may be significantly apparent on tram lines, especially, on the curves located on street intersections. In case of wheel–rail lubrication, there is a risk of braking force reduction close to the stations or platforms located on curves.

Radial wheelset steering can be implemented in its simplest form by means of selecting specific longitudinal stiffness characteristics (lower values) of the primary suspension [4]. In fact, reducing longitudinal stiffness entails lower critical speed. Nevertheless, usually, the rail vehicles operating on metro or tram lines are not intended to achieve high speeds; therefore, its suspension could have softer characteristics.

The more complex radial steering systems are divided into two groups [2, 5-7]:

- passive – incorporate links and levers that are activated, e.g. as result of relative motions of bogies and the body;
- active – mechatronic solutions composed of actuators.

The passive radial steering mechanisms are not common because of their complexity and higher cost. Moreover, operation of passive steering devices is insufficient in the transition curves [8]. An active element enabling improvement of wheelset steerability is in the prototype phase.

In the search for solutions to improve the wheel–rail interaction on tight curves, the numerical study of a tractive metro vehicle with wheelsets equipped with differential gears was carried out. In the recent literature the problem of differentials in the rail vehicles was examined by Wu [9], albeit only the bogie model was studied. A differential is also implemented in a prototype of the ‘Brems-tram’ [10]. More generally, bogies with differential gears can be considered as a part of a wider group of unconventional running gears, represented mainly by wheelsets with independently rotating wheels (IRW). Dynamic and kinematic properties of vehicles with IRW have been extensively studied [11-14] as have been its control techniques in e.g. [15].

The paper concerns a dynamic behavioral study of one segment of the metro car model with differentials according to proposed simulation scenarios.

2. VEHICLE MODEL

In order to investigate the influence of a differential gear on rail vehicle dynamics a simulation model was built in VI-Rail (former Adams/Rail) simulation package. The philosophy of creating a model in the software is based on the standard assumptions of multi-body modelling [16, 17]. The vehicle’s general inertial elements are rigid and connected by means of massless springs and dampers. However, some approaches to multi-body modelling may also be supplemented with flexibility of the inertial elements [18]. The created model derives its topology and parameters (inertial, geometrical and suspension characteristics) from a typical, modern metro tractive segment (one body-piece), which operates on the second line of Warsaw Metro. Selected parameters of the vehicle model are presented in Tab. 1.

The simulation software derives the Euler–Lagrange equation of motion to model the behaviour of its main inertial elements (wheelsets, bogies and body) interconnected with joints. The motion of the vehicle model is a result of the forces generated in a wheel–rail contact patch and inertial forces. Motion constraints of the wheelset originate from its interaction with a rigid track model. The constraints are non-linear and depend on the geometric parameters of the wheelset and track, i.e. track gauge, cant, wheel and rail profiles, distance between contact patches, etc.

Table 1

Selected parameters of the metro vehicle model

Parameter	Value	Units
Wagon base	12.6	[m]
Bogie base	2.1	[m]
Wagon mass	29000	[kg]
Body mass	15400	[kg]
Wheelset mass	1672	[kg]
Nominal wheel diameter	0.85	[m]
Lateral stiffness of one primary spring	3507.4	[kN/m]
Lateral stiffness of one secondary spring	79.4	[kN/m]
Vertical stiffness of one primary spring	470	[kN/m]
Vertical stiffness of one secondary spring	345	[kN/m]
Damping coefficient of primary suspension, x, y, z	3	[kNs/m]
Damping coefficient of secondary suspension, x, y, z	2	[kNs/m]

Calculation of the wheel–rail contact forces has been an aim of extensive studies [19] because of difficulties originating in non-linear profiles of a wheel tread and rail head in the contact patch. The contact forces provide wheelset lateral guidance in track, are responsible for reactions due to vertical load, traction forces, etc. Models of wheel–rail contact enable calculation of tangential and normal forces generated in the contact patch of two elastic bodies during their rolling with creep.

Mathematical description of the wheel–rail interaction is complex because of the fact that all contact parameters depend strongly on the wheel and rail geometry, and that, in some circumstances, multiple points of contact may occur. The study of contact between the wheel and rail can be generally divided into two tasks [19]:

- normal task – calculation of number, location and dimensions of a contact patch and normal pressure distribution;
- tangential task – calculation of tangent stresses and tangent force values arising because of friction and creepages in the contact area.

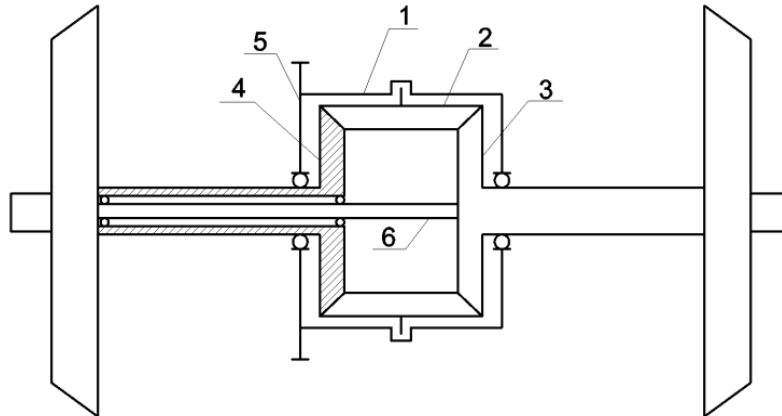
The most common algorithm for contact force calculation is FASTSIM by J.J. Kalker [20]. It is a simplified CONTACT algorithm, also developed previously by Kalker. The FASTSIM is based on the ‘stripes theory’. It is limited to an elliptical contact patch, making some assumptions similar to Hertz’s contact theory:

- contact area is elliptical and flat stress distribution is elliptical;
- creepages are calculated relative to the geometric centre of the ellipse;
- elliptical contact area is divided into parallel longitudinal stripes of Δy_i width and length along the x axis depending on the ellipse size;
- all stripes are divided into the same number of elements and stress calculation is initiated from the ellipse edge;
- Kalker’s c_{ij} coefficients are constant on the entire contact patch;
- Local deformations refer to the local force.

The VI-Rail simulation software utilizes the modified FASTSIM algorithm, which enables calculation of the total normal force, the applied traction forces, creepages, actual rolling radius, etc. The adopted algorithm computes contact parameters at each simulation step, contrary to utilizing contact tables with predefined Kalker’s coefficients.

The vehicle model was built in two versions – the first one with conventional wheelsets, and the second one with differential gears at each wheelset. The differential gear is placed in the housing of the reduction gear, which transmits tractive torque from the motor. The scheme of a differential wheelset is depicted in Fig. 1. The rail wheelset is subject to high vertical and lateral loads, and also to bending moments. In the conventional wheelset, an axle transmits the bending moment. As the

differential splits the axle into two separate driveshafts the differential housing would be loaded by a substantial bending moment. To reduce load on the housing, the hollow driveshafts are proposed to be mounted on a common axis by means of rolling bearings (Fig. 1).



1 – Pinion carrier; 2 – Pinion; 3, 4 – Right/left output gear with hollow shaft; 5 – Ring gear; 6 – Supporting axle

Fig. 1. The idea of a differential wheelset

Equation 1, governing splitting of the angular velocity of a symmetrical differential, is derived from the Willis formula on planetary gears. If the left wheel is accelerated and gains angular velocity $+\Delta\omega_L$, the right wheel is decelerated by $-\Delta\omega_R$ value.

$$\omega_0 = \frac{\omega_L + \omega_R}{2} \quad (1)$$

where: ω_0 is angular velocity of differential housing (pinion carrier), ω_L , ω_R are angular velocities of the left and right output gears.

To supplement the description of differential operation we also need to introduce an equation defining torque splitting (Equation 2-3). For a symmetrical differential input, torque τ_0 is divided equally for both output gears. In the case of an idealized open differential, there is no internal friction torque. However, in a real differential internal friction cannot be eliminated, but it can also be increased intentionally to shift the threshold of differential activation. Friction torque τ_f causes output gears (wheels) to rotate at the same angular velocity (like a conventional wheelset) unless the difference of torques is $\tau_L - \tau_R = 2\tau_f$.

$$\tau_0 = \tau_L + \tau_R \quad (2)$$

$$\tau_L = \tau_0 - \tau_f; \quad \tau_R = \tau_0 + \tau_f \quad (3)$$

One of the disadvantages of a differential is limiting traction in some particular circumstances. When negotiating curves, the inner wheel may be unloaded because of inertial force. The torque transmitted by the outer wheel (loaded by normal component of inertial force) is then limited to the value of the inner wheel. The total tractive effort of a differential wheelset is lower than that in the case of a conventional wheelset. The reduction of tractive force is also possible if the coefficient of friction between one wheel and rail is lower than in the opposite contact patch. However, in the case of a railway, the difference between friction coefficients of the left and the right wheel–rail contact patches could appear to be lower than that in the case of a tyre–road pair. Therefore, the last condition may not play a significant role in generating a tractive or braking effort of the rail vehicles with differential gears.

3. SIMULATION CONDITIONS

Complete testing of a rail vehicle from the dynamic point of view is carried out according to the UIC leaflet [21] and European norms [22]. The scope of the prescribed tests is established to assess

typical rail vehicles with conventional running gears for the homologation process. However, the vehicles with unconventional running gear should also comply with these documents in order to be put into service. Nevertheless, the normative scenarios are not designed to investigate the specific behaviour of such vehicles. The researchers of rail vehicles with unconventional running gears create specific simulation scenarios to carry out more effective observation [23, 24]. The special scenarios may include passage on a low-radius curve, track buckling or gauge narrowing.

To obtain information on influence of a differential on dynamic behaviour and wear, two simulation scenarios are proposed:

- scenario 1 – a track with low-radius curve, $R=100$ m;
- scenario 2 – a track with $R=600$ m curve.

Geometric parameters of the tracks' longitudinal profiles in the above scenarios are depicted in Tab. 2. In both scenarios the implemented rail profile is UIC 60, rail inclination equals to 1:40 and zero cant.

Table 2

Parameters of the track used in Scenario 1

No.	Section geometry	Section length	
		Scenario 1	Scenario 2
1	tangent	$l_1 = 100$ m	$l_1 = 100$ m
2	transition curve	$l_2 = 20$ m	$l_2 = 50$ m
3	regular curve	$l_3 = 100$ m ($R=100$ m)	$l_3 = 400$ m ($R=600$ m)
4	transition curve	$l_4 = 20$ m	$l_4 = 50$ m
5	tangent	$l_5 = 100$ m	$l_5 = 100$ m

The differentials at each wheelset in the vehicle model transmit tractive torque, which is balanced by resistive torque applied to wheels. Resistive torque value is calculated based on Equation 4 describing resistive force acting on a multiple unit [25]. The equation was developed by Railway Institute (Poland).

$$R = (0.65 + 0.054v)Q + 147n + (2.7 + z) \cdot 1.271v^2 \quad [\text{N}] \quad (4)$$

where Q is vertical load of the unit [kN] (285 kN); z is number of body pieces of the unit (1 segment assumed); n is number of wheelsets (4); v is speed [m/s].

The effects of a differential on rail vehicle dynamics are investigated by means of kinematic values, such as wheelset lateral displacement, or angle of attack, and force values (lateral forces). As the differential is expected to reduce guiding forces in tight curves, this fact could entail lower wear of wheels and rails. A measure of wheel wear used in the study is Wear number based on $T\gamma$ wear model [26, 27]. The basic assumption of this model is proportional dependence of worn material and dissipated energy in the wheel–rail contact [28]. The Wear number is expressed by Equation 5:

$$W_n = \frac{1}{A} \frac{\mu}{0.6} (T_x v_x + T_y v_y) \quad [\text{Nm/m}] \quad (5)$$

where A is area of wheel–rail contact patch; μ is wheel–rail coefficient of friction ($\mu = 0.4$ adopted); T_x , T_y is longitudinal and lateral tangent contact force; v_x , v_y is longitudinal and lateral relative slip.

The internal friction torque of the differential gears was set to several consecutive values, starting from 0 Nm (open differential) up to 2000 Nm for each simulation scenario. The intention of implementing friction torque is providing proper running behaviour on a tangent track. As it is proved in section 4, differential wheelsets do not provide self-steering ability. If a differential wheelset is shifted laterally from its central position, then it does not return like a conventional wheelset. As both wheels are not rigidly linked together, the creep forces do not cause wheels to move towards the centreline. From this point of view an open differential wheelset acts like a wheelset with IRW [11, 29].

4. SIMULATION STUDY

Conventional and differential wheelsets of the metro wagon model are shifted laterally at the initial phase of simulation in both scenarios. It is caused by the fact that a heavy mass (over 400 kg), representing reduction gear with a differential, is not located in the wheelset's geometric centre. The self-steering ability of a conventional wheelset enables travelling along the track centreline with initial hunting oscillations that vanish after ca. 20 m at $v = 20$ km/h. No hunting oscillations are observed in the case of a wheelset with an open differential; however, its lateral displacement increases up to ca. 3.5 mm until it reaches the first transition curve. The differential wheelset responds similarly to the wheelset with IRW. Thus, on a tangent track section this feature is considered a disadvantage because of prolonged flange–rail contact and a higher risk for derailment (Fig. 2). The improvement of running on a straight track is possible to achieve by means of programming internal friction torque. For $\tau_f = 1000$ Nm, hunting oscillation occurs, contrary to the open differential, and tends to vanish completely after ca. 50 m (Fig. 2 – left).

During steady curving, the peak lateral displacement of the leading wheelset of the first bogie is the same for each tested solution. For the trailing wheelset, both types of differential caused a minor increase in lateral displacement (Fig. 2 – right).

A comparison of angles of attack is presented in Fig. 3. For the leading wheelset there are no relevant changes in the peak angles. The trailing wheelset with differential gears (open and with friction) is subject to slightly higher angles of attack – differential wheelset radial steering ability is slightly reduced in this scenario.

The influence of the differential on lateral forces exerted in the wheel–rail contact is depicted in Fig. 4. At $v = 20$ km/h in scenario 1, much lower guiding forces (ca. 7 kN) are exerted in the contact patch of the outer wheel of the differential wheelset (both types). However, we can expect that at higher speeds the outer wheel would be additionally loaded by the normal component of the inertial force, and the differential may not bring any benefits in such conditions.

In the case of a differential wheelset, Wear number of the outer wheel is lower (Fig. 5a – left), and it can be concluded that the differential reduces negative effects associated with negotiating tight curves.

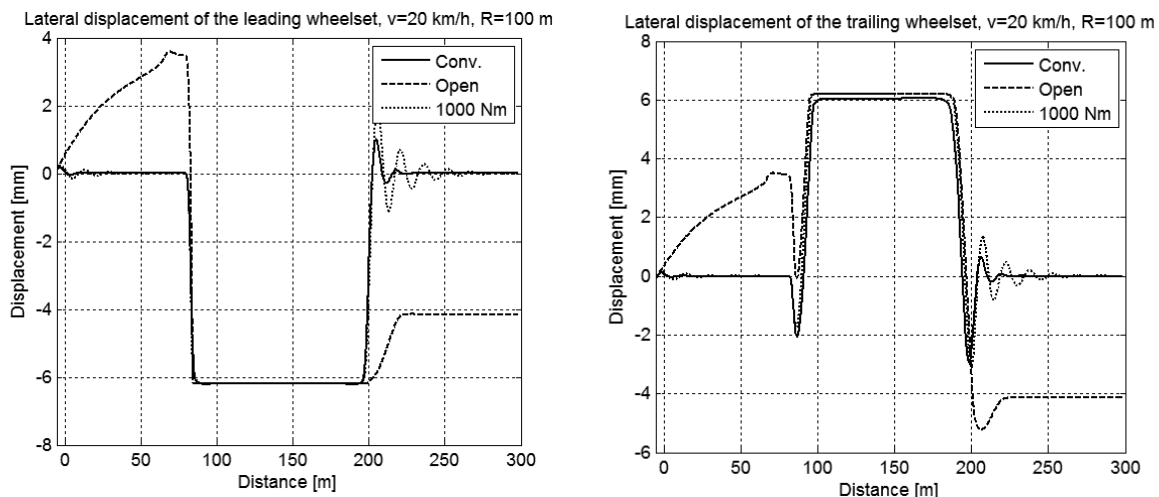


Fig. 2. Lateral displacement of the leading and trailing wheelset, $v = 20$ km/h, $R = 100$ m

During steady curving, the increase of lateral forces occurs in the inner wheel–rail contact patch for a differential wheelset (ca. 1.5 kN). Wear number of the inner wheel is practically the same for both solutions of the running gear (Fig. 5b – right).

As the trailing wheelset with a differential gear operates at higher angles of attack, the lateral forces of both wheels are higher (Fig. 6), especially, in the case of the outer wheel (up to ca. 12 kN, Fig. 6 – left). Nonetheless, despite much higher lateral forces, wear number of both wheels of the trailing wheelset are significantly lower: particularly, in the case of the outer wheel of the conventional

wheelset (Fig. 7). The reason for this non-intuitive phenomenon may lay in the higher values of longitudinal creepages or forces generated in the wheels of the conventional wheelset.

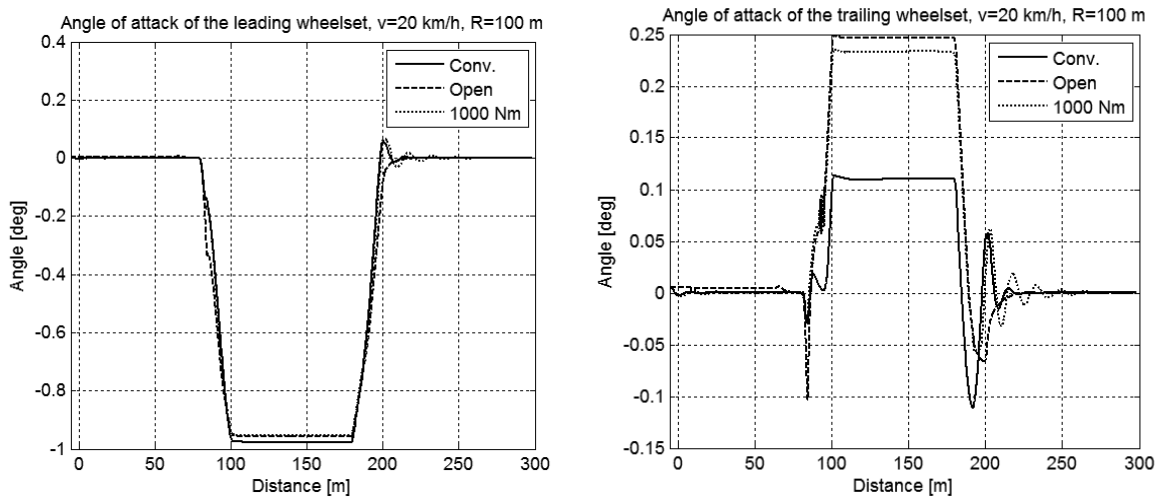


Fig. 3. Angle of attack of the leading and trailing wheelset, $v = 20$ km/h, $R = 100$ m

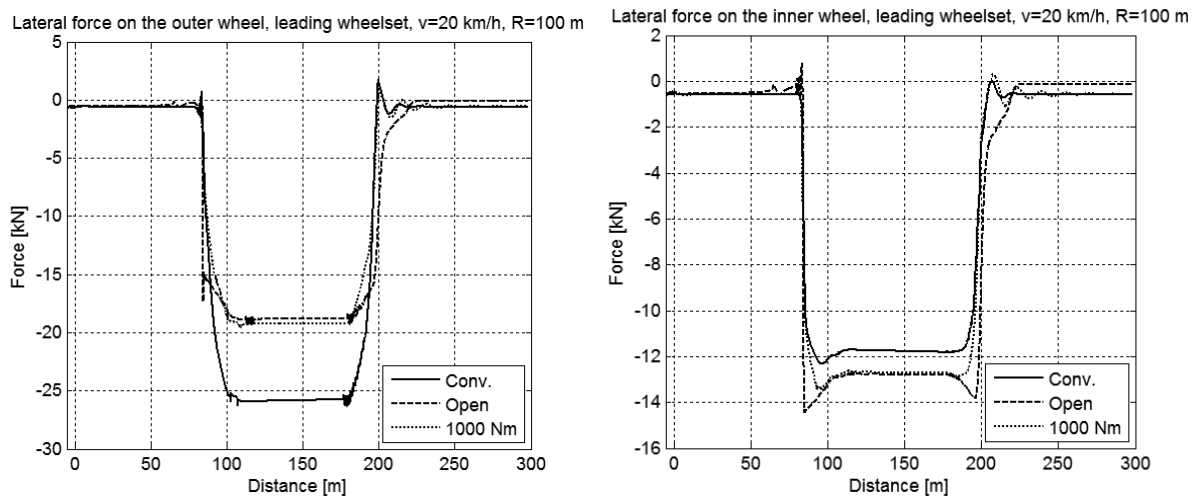


Fig. 4. Lateral forces on the outer and the inner wheel of the leading wheelset, $v = 20$ km/h, $R = 100$ m

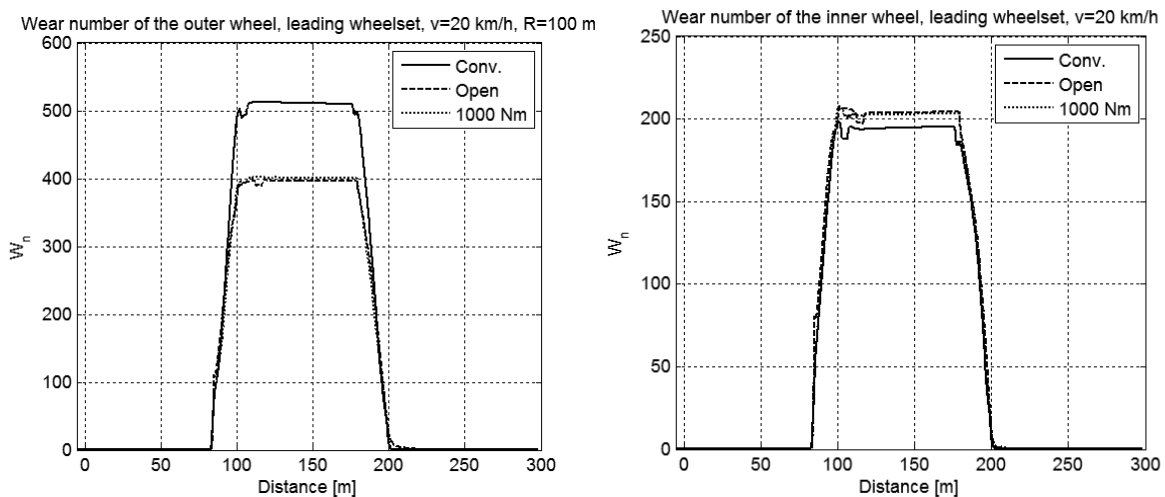


Fig. 5. Wear number – the outer and the inner wheel of the leading wheelset, $v = 20$ km/h, $R = 100$ m

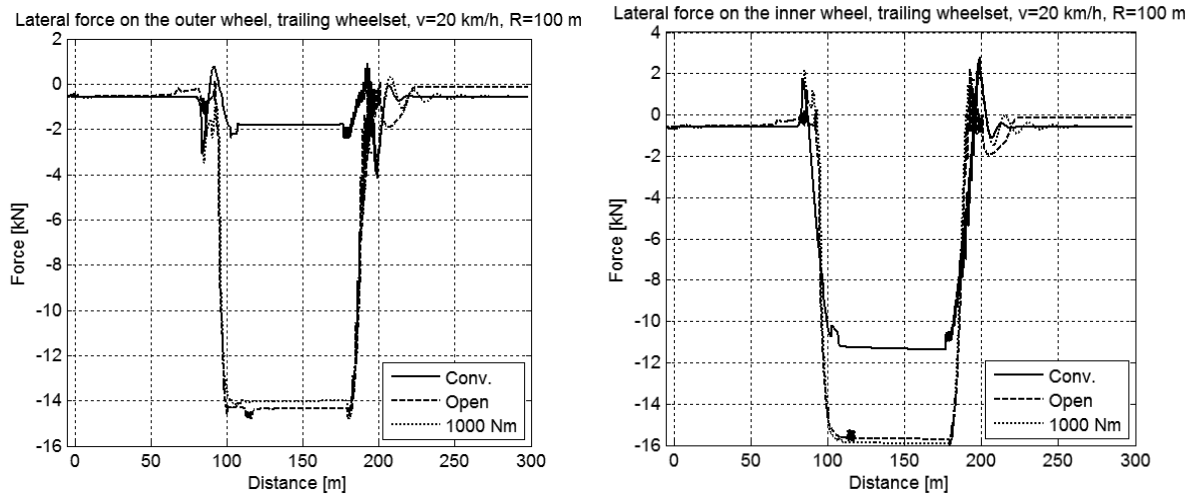


Fig. 6. Lateral forces on the outer and the inner wheel of the trailing wheelset, $v = 20$ km/h, $R = 100$ m

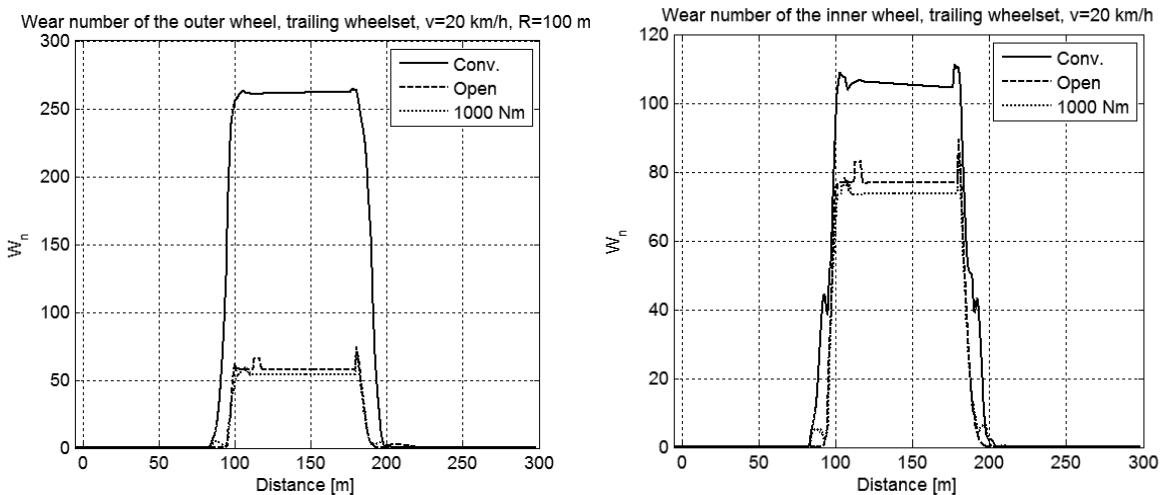


Fig. 7. Wear number – the outer and the inner wheel of the trailing wheelset, $v = 20$ km/h, $R = 100$ m

The value of the fixed friction torque has an effect on wheelset hunting oscillations. Low hunting is initiated at the beginning of the first tangent section. Exiting the curve induces substantial oscillations. With an increasing value of friction torque the oscillations are damped at a shorter distance.

Fig. 8 depicts logarithmic decrement of wheelsets' hunting oscillations for the curve-exiting case of scenario 1. Apart from the torque value, the damping of hunting also depends on vehicle speed. For $v = 50$ km/h logarithmic decrement values are evidently higher. However, the greater speed value is rather unsafe for the designed scenario track. In the case of safe speed ($v = 20$ km/h), there is no significant effect of increasing friction torque value over 1000 Nm as the value of logarithmic decrement is saturated. In the case of $\tau_f = 40$ Nm decrement has a negative value: the oscillation amplitude tends to increase.

As increasing friction torque value helps reduce hunting, it does not have much influence on the lateral force change of the inner wheel compared with the conventional wheelset. In the considered scenario $\tau_f = 40$ Nm reduces guiding force value (during steady curving), practically, as in the case of $\tau_f = 2000$ Nm for both travelling speeds (Fig. 9). The lateral forces exerted in the outer wheel–rail contact patch are lower for a differential wheelset for low speed (20 km/h). However, a substantial attenuation of the decrease is apparent starting from $\tau_f = 1000$ Nm. At $v = 50$ km/h the high inertial forces push the wheelset towards the outer rail, which, in turn, results in the increase of the lateral forces, regardless of the programmed friction torque.

The results of the scenario 2 analysis are presented in the form of Wear number value plots (Fig. 10). Because of the higher curve radius, W_n values are very low compared with scenario 1 (for both speeds). The proposed solution does not show any advantage over the conventional solution on a track with a greater curve radius: the differential (open and with friction) causes slightly higher wear on both wheels.

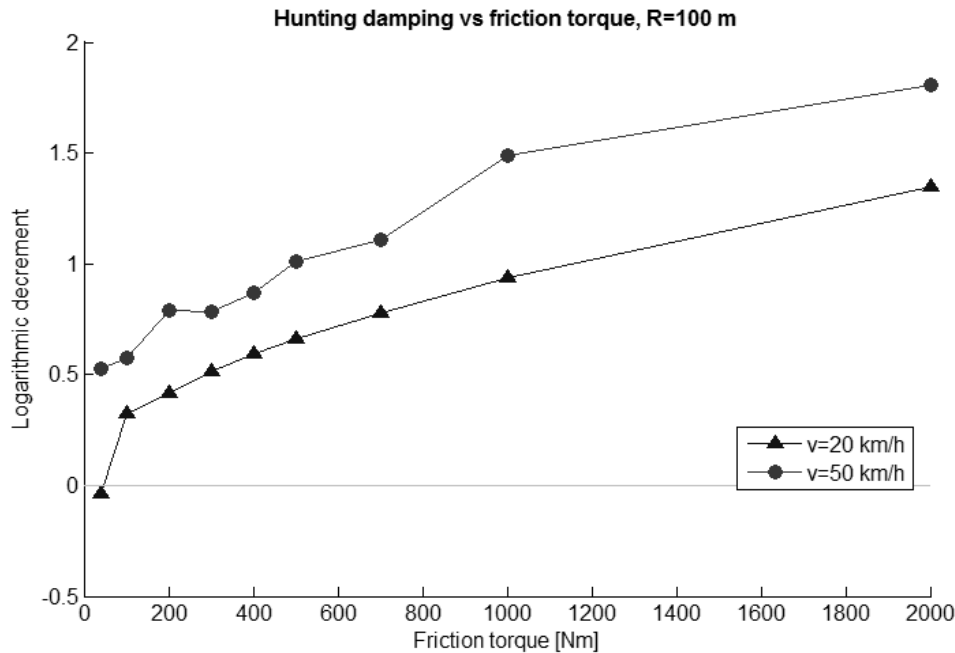


Fig. 8. Hunting damping dependence on internal friction torque

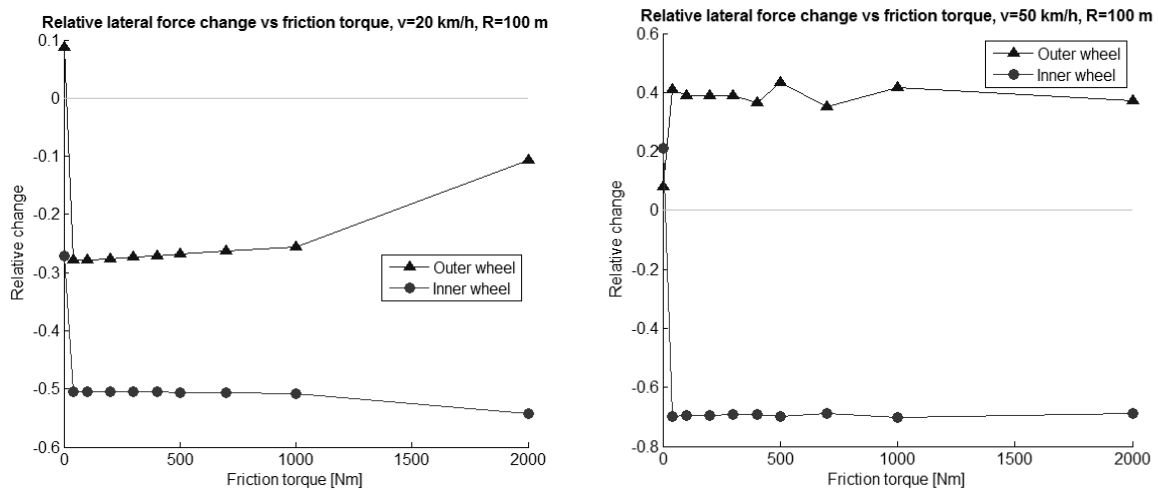


Fig. 9. Relative lateral force change vs friction torque, $v = 20$ km/h and $v = 50$ km/h, $R = 100$ m

5. CONCLUSIONS

The aim of the study was to examine the dynamic behavior of the metro vehicle model equipped with differentials. The use of a differential was intended to improve the interaction of the constrained wheelsets (in the bogies) with rails in tight curves.

The simulation results indicated that the positive effects of a differential wheelset could occur in a narrow range of conditions, mainly on sharp curves. In these particular circumstances, a vehicle equipped with the differential shows an advantage over the conventional setup. The vehicle model with differentials is subject to lower lateral forces during curving. Estimated wear of the wheels of the

differential wheelset is generally lower according to the implemented wear model. Curve negotiation was improved in scenario 1 ($R = 100$ m) compared with the conventional wheelset.

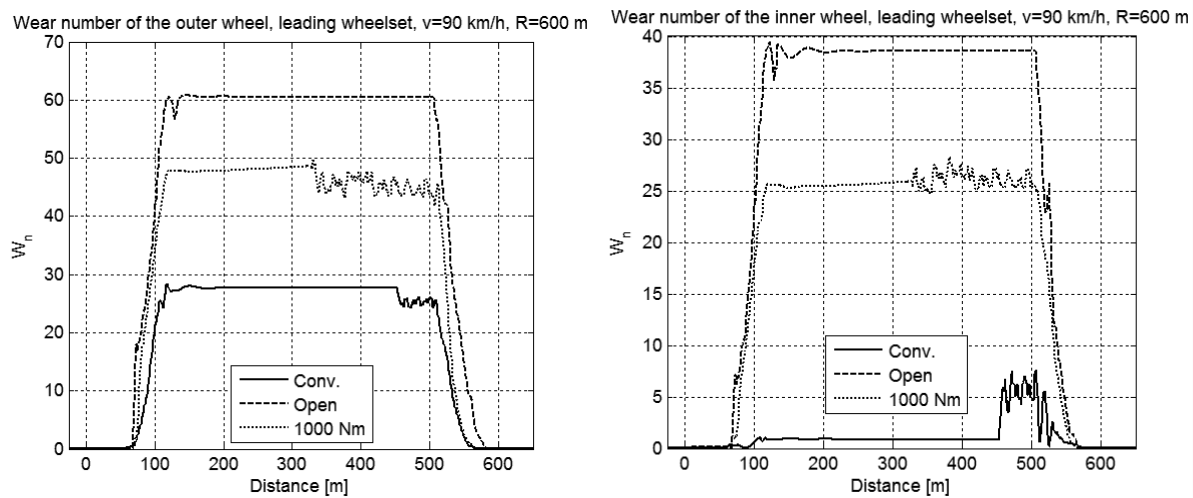


Fig. 10. Wear number – the outer and the inner wheel of the leading wheelset, $v = 90$ km/h, $R = 600$ m

In the case of a curve of greater radius – 600 m – the differentials worsen running abilities of the vehicle. The increase of lateral forces and higher wear are evident, particularly, for the differential without friction.

The wheelset with an open differential does not possess a self-steering ability, which is of great importance. Thus, it exhibits the same disadvantage as a running gear with independently rotating wheels. In order to preserve self-steering, but with a longer wavelength of hunting oscillation, an internal friction torque should be programmed. Further, the results have shown that relative changes in lateral forces are not highly dependent on the friction torque value in the considered simulation scenarios. For the tested vehicle the fixed value of $\tau_f = 1000$ Nm can be adopted for normal operation. This value enables hunting oscillations and its damping similarly to the conventional wheelset. Moreover, it also provides greater decrease of lateral force in the outer wheel compared with higher τ_f values.

The potential use of a differential in light rail vehicles may be limited to the vehicles operating on the lines with numerous low-radii curves ($R = 50 \div 150$ m). In the curves of higher radii, a differential (particularly, an open one) increases wear; however, the difference in wear is small compared with the benefits achieved on sharper curves.

Acknowledgement

This work was supported by the Dean's Research Grant (2016): 'The simulation study of a tractive metro vehicle equipped with differential gears' at Warsaw University of Technology [504/02625/1160/42.000100].

References

1. Redtenbacher, F.J. *Die gesetze des locomotiv-baues*. Verlag von Friedrich Bassermann. 1855. 328 p.
2. Iwnicki, S. *Handbook of railway vehicle dynamics*. Taylor & Francis. 2006. 548 p.
3. Piotrowski, I. A Theory of wheelset forces for two point contact between wheel and rail. *Vehicle System Dynamics*. 1982. Vol. 11. No. 2. P. 69-87.

4. Andersson, E. & Orvnäs, A. & Persson, R. On the optimization of a track-friendly bogie. In: *Proceedings of the 21st International Symposium on Dynamics of Vehicles on Roads and Tracks, IAVSD'09*. Stockholm, August 17-21. 2009. P. 1-13.
5. Sato, E. & Kobayashi, H. & Okamoto, I. & Tezuka, K. & Kakinuma, H. & Tamaoki, T. Lateral force between wheel and rail during curve negotiation of a limited express diesel car with forced steering bogie. *Vehicle System Dynamics*. 2002. Vol. 37. Supplement 1. P. 678-689.
6. Matsumoto, A. & Sato, Y. & Ohno, H. Curving performance evaluation for active-bogie-steering bogie with multibody dynamics simulation and experiment on test stand. *Vehicle System Dynamics*. 2009. Vol. 46. Supplement 1. P. 191-199.
7. Michalek, T. & Zelenka, J. Reduction of lateral forces between the railway vehicle and the track in small-radius curves by means of active elements. *Applied and Computational Mechanics*. 2011. Vol. 5. P. 187-196.
8. Sato, E. & Kobayashi, H. & Tezuka, K. Lateral force during curve negotiation of forced steering bogies. *Quarterly Report of Railway Technical Research Institute*. 2003. Vol. 44. No. 1. P. 8-14.
9. Wu, X. & Chi, M. & Zeng, J. & Zhang, W. & Zhu, M. Analysis of steering performance of differential coupling wheelset. *Journal of Modern Transportation*. 2014. Vol. 22. No. 2. P. 65-75.
10. Kolář, J. Design of a Wheelset Drive. *Transactions on Electrical Engineering*. 2015. Vol. 4. No. 1. P. 11-19.
11. Eickhoff, B. M. 1991. The application of independently rotating wheels to railway vehicles. In: *Proceedings of the Institution of Mechanical Engineers, Part F: Journal of Rail and Rapid Transit January*. 1991. Vol. 205. No. 1. P. 43-54.
12. Fiset, P. & Samin, J.C. Lateral dynamics of a light railway vehicle with independent wheels. *Vehicle System Dynamics*. 1992. Vol. 20. Supplement 1. P. 157-171.
13. Liang, B. & Iwnicki, S. An experimental study of independently rotating wheels for railway vehicles. In: *Proceedings of the International Conference on Mechatronics and Automation ICMA 2007*. Harbin, China, 5-8 Aug. 2007. P. 2282-2286.
14. Opala, M. Study of the derailment safety index Y/Q of the low-floor tram bogies with different types of guidance of independently rotating wheels. *Archives of Transport*. 2016. Vol. 38. No. 2. P. 39-47.
15. Dolecek, R. & Cerny, O. & Nemecek, Z. The sophisticated routing control of the bogie. In: *14th Biennial Baltic Electronics Conference (BEC2014)*. Tallinn. 2014. P. 233-235.
16. Shaltout, R. & Ulianov, C. & Baeza, L. Development of a simulation tool for the dynamic analysis of railway vehicle - track interaction. *Transport Problems*. 2015. Vol. 10. Special Edition. P. 47-58.
17. Dižo, J. & Blatnický, M. Use of multibody system dynamics as a tool for rail vehicle behavior diagnostics. *Diagnostyka*. 2016. Vol 17. No. 2. P. 9-16.
18. Dižo, J. & Blatnický, M. Computer analysis of a wagon bogie running with a flexible frame. In: *Proceedings of the XVII Scientific-Expert Conference on Railways RAILCON'16*, Nis, Serbia. 13-14 October 2016. P. 37-40.
19. Bosso, N. & Spiriyagin, M. & Gugliotta, A. & Soma, A. *Mechatronic modeling of real-time wheel-rail contact*. Springer-Verlag Berlin Heidelberg. 2013. 119 p.
20. Kalker, J.J. A fast algorithm for the simplified theory of rolling contact. *Vehicle System Dynamics*. 1982. Vol. 11. No. 1. P. 1-13.
21. UIC 518:2009. Testing and approval of railway vehicles from the point of view of their dynamic behaviour – Safety – Track fatigue – Ride quality. International Union of Railways (UIC) Leaflet.
22. EN 14363:2016. Railway applications – Testing and simulation for the acceptance of running characteristics of railway vehicles. Running behaviour and stationary tests. European Standard.
23. Chudzikiewicz, A. & Sowińska, M. 2015a. Low-floor trams running gear – comparative simulation studies. In: *Proceedings of the 14th Mini Conference on Vehicle System Dynamics, Identification and Anomalies, VSDIA 2014*. Budapest, Hungary. 10-12 November 2014. P. 203-210.
24. Chudzikiewicz, A. & Sowiński, B. & Stelmach, A. & Wawrzyński, W. Simulation analysis and comparison regarding vibration of conventional and nonconventional wheelsets. In: *Proceedings*

- of the 22nd International Congress on Sound and Vibration*. Florence, Italy. 12-16 July 2015. P. 1–6.
25. Madej, J. *Teoria ruchu pojazdów szynowych*. Oficyna Wydawnicza Politechniki Warszawskiej. 2004. 124 p. [Madej, J. *Theory of rail vehicle traffic*. Publishing House of the Warsaw University of Technology]
 26. Jendel, T. & Berg, M. Prediction of wheel profile wear. *Vehicle System Dynamics*. 2002. Vol. 37. Supplement 1. P. 502-513.
 27. Lewis, R. & Braghin, F. & Ward, A. & Bruni, S. & Dwyer-Joyce, R.S. & Bel Knani, K. & Bologna, P. Integrating dynamics and wear modelling to predict railway wheel profile evolution. In: *Proceedings of the 6th international conference on contact mechanics and wear of rail/wheel system*. Gothenburg, Sweden. 10-13 June 2003. P. 7-16.
 28. Enblom, R. Deterioration mechanisms in the wheel-rail interface with focus on wear prediction: A literature review. *Vehicle System Dynamics*. 2009. Vol. 47. No. 6. P. 661-700.
 29. Dukkupati, R.V. & Swamy, S.N. & Osman, M.O.M. Independently rotating wheel systems for rail vehicles-a state of the art review. *Vehicle System Dynamics*. 1992. Vol. 21. No. 1. P. 297-330.

Received 11.02.2016; accepted in revised form 29.08.2017